IEEE Access
Multidisciplinary | Rapid Review | Open Access Journal

Received 25 June 2024, accepted 8 July 2024, date of publication 15 July 2024, date of current version 23 July 2024.

Digital Object Identifier 10.1109/ACCESS.2024.3427651

RESEARCH ARTICLE

Posture Estimation in Agriculture: Employing Inertial Measurement Units and Unscented Kalman Filtering for Trunk, Shoulder, and Elbow Analysis

AMINE ZOUGALI AND ORNWIPA THAMSUWAN
Department of Mechanical Engineering, École de Technologie Supérieure, Montreal, QC H3C 1K3, Canada

Corresponding author: Ornwipa Thamsuwan (ornwipa.thamsuwan@etsmtl.ca)

This work was supported in part by the École de Technologie Supérieure, Start-Up Fund for New Professor; and in part by the Natural Sciences and Engineering Research Council of Canada (NSERC) Discovery under Grant RGPIN-2022-03927.

This work involved human subjects in its research. Approval of all ethical and experimental procedures and protocols was granted by the Research Ethics Committee of the École de technologie supérieure, under Application No. H20211103, and performed in line with the Declaration of Helsinki.

ABSTRACT Farmworkers are often at risk of musculoskeletal health problems, with low back pain being the most common, accounting for approximately over half of the population worldwide. Moreover, these musculoskeletal disorders (MSD) are prevalent in other body regions including shoulders, elbows, wrists or hands. As these issues were found related to inappropriate working postures, it is beneficial to quantify these postures in order to prevent work-related MSD. The primary focus of this study was to improve the estimation of the postures and the exposure to non-neutral postures among agricultural workers. Three inertial measurement units (IMU) were attached to the upper back, upper arm, and forearm of nine workers while they were performing their regular work activities. A posture characterization algorithm was developed to rely on the data from only accelerometers and gyroscopes while excluding magnetometer readings due to high magnetic disturbance. Despite these challenges, a specialized unscented Kalman filter (UKF) was developed to achieve a more precise posture estimation. The UKF effectively expanded the range of pitch angles from ± 90 degrees to ± 180 degrees, resulting in a substantial improvement in the assessment of the back inclination as well as shoulder and elbow angles. The study was carried out among workers in a large-scale plant nursery, revealing instances of extreme postures in the back, upper arms, and elbows during their work activities. The quantitative findings highlighted the high exposure to ergonomic risks faced by the workers. This emphasized the urgent need for implementing appropriate measures to mitigate these risks.

INDEX TERMS Agriculture, inertial sensor, human posture, sensor fusion algorithms, unscented Kalman filter.

I. INTRODUCTION

In the agricultural sector, many workers struggle with musculoskeletal disorders (MSD), especially the low back pain, which was estimated to have 50% greater prevalence than those in other sectors. Furthermore, other body parts such as shoulders, elbows, wrists and hands manifested a 20% higher prevalence as compared to non-agricultural workers [1], [2]. Low back pain has been the most common pain site, affecting 39% of individuals in the United States [3], and was ranked as the second most frequent reason for medical consultations. Approximately half of the American workforce reported experiencing back pain symptoms annually, and these estimates suggested that around 80% of people would experience back problems during their lifetime [4], [5]. Additionally, MSD injuries contributed to 12% of morbidity and absences from work, resulting in a significant economic and social burden [2]. In the U.S., the

The associate editor coordinating the review of this manuscript and approving it for publication was Emanuele Lattanzi.

economic cost of pain in 2010 ranged from 560 billion to 635 billion (100 billion exclusively for back pain) [6], with an expected upward trajectory [7]. Similarly, in Canada, expenses reached between 6 and 12 billion dollars in 2014 [2], [8].

Agricultural activities often require workers to be engaged in strenuous muscular exertion, non-neutral work postures, and rapid and repetitive movements [9], [10]. An epidemiological study showed that these are some examples of the risks contributing to the development of MSD [11]. In general, these risk factors can be broadly categorized into three main groups: intrinsic factors related to the body, external factors related to the environment, and task-related factors related to the nature of the task itself [12]. This categorization can be used to formulate recommendations to improve the ergonomics of agricultural tasks, reducing the risk of injury and promoting the well-being of workers in the agricultural sector.

In order to better understand these factors, it is crucial to analyze the relevant postures such as trunk flexion and lateral bending, shoulder flexion and abduction, and the angles of upper extremity joints of individuals during their work tasks in real-world environment. Traditionally, postures can be characterized using methods such as OWAS [13], RULA [14] and REBA [15], [16]. Based on the RULA and REBA techniques, the hazardous postures of trunk inclination (concerning both trunk flexion and lateral bending) and shoulder angles are over 60 and 90 degrees, respectively. However, these methods are subjective to the view of the observers. Nowadays, the use of technology such as accelerometers, inertial measurement units (IMU) and motion capture system [17] was proven to effectively reduce these human errors. The use of these sensors placed on targeted body parts provides basic parameters such as tri-axial accelerations and angular velocities of the human body segments during rehabilitation [18] and work activities in agriculture or any other industries. After that, the data need to be processed using specialized algorithms such as sensor fusion and the application of rotation matrix to estimate postures or joint angles.

In this introduction section, the state-of-the-art of the wearable sensors and the fusion algorithms are presented, and followed by the objectives of this study.

A. THE USE OF THE IMU AS MEASUREMENT DEVICE

IMU combines accelerometers, gyroscopes and magnetometers, which can provide essential data including linear accelerations, angular velocities and magnetic field strength to determine an object's orientation and movements in a three-dimensional space. The ability to function without external references makes IMUs particularly valuable for detailed kinematic analysis. However, each sensor in the IMU has specific error characteristics that can impact the accuracy of posture estimation [19], [20]. First, accelerometers are sensitive to high-frequency movements, limiting their capability in capturing rapid changes in acceleration [21], [22], i.e., measurements are consistently shifted away from the true values. This can occur due to calibration mistakes or differences in the manufacturing process.

In addition, gyroscopes can produce readings that drift over time, even when the object is stationary. This can be caused by changes in temperature or external vibrations [23], [24]. In reality, there are manufacturing imperfections that can cause mismatches in frequencies and quality factors in resonators [25]. These discrepancies can result in drift and locking of oscillation angles. Although integrating gyroscope data with accelerometer data can reduce high-frequency noise, thus making the output more stable, the yielded angles are still potentially biased. In other words, this process can accumulate low-frequency components from the noise, leading to drift in gyroscope readings over time. This is a well-recognized challenge when using gyroscopes for long-term orientation estimation [22], [25], [26], [27].

Lastly, magnetometers can introduce errors due to their biases, scale factor variations, and susceptibility to magnetic disturbances [28], [29], often necessitating a calibration during setup, which can be challenging in real-time scenarios. Calibrating for hard and soft iron effects is crucial to enhance accuracy [30]. Moreover, magnetic disturbances from nearby electronic devices or metal objects can further disrupt measurements, leading many sensor fusion algorithms to exclude magnetometers, especially in locations prone to such disturbances. The decision to include or exclude magnetometers revolves around balancing their potential benefits with the risk of introducing errors [22], [28], [31]. To address these aforementioned issues on the sensors, various strategies were developed like magnetic field rejection [32], [33], [34], zero velocity updating [35], [36] and kinematic modeling [37], were implemented alongside sensor fusion algorithms [38], [39].

B. SENSOR FUSION ALGORITHMS

Despite ongoing research and hardware improvements, IMU-based systems struggle to capture prolonged, full three-dimensional motion in unconstrained environments [40]. Rather than using a standalone accelerometer, gyroscope or magnetometer, it is often necessary to combine data from IMU sensors using one or more sensor fusion algorithms. These algorithms take into account the strengths and weaknesses of each sensor, and employ mathematical models to integrate sensor data and correct errors and biases [41]. Various sensor fusion algorithms may be used, such as Madgwick's filter [42], [43], complementary filters [43], [44], Kalman filter [40], [45], extended Kalman filter [46], [47], [48] and particle filters [34]. These algorithms offer different levels of precision and complexity, depending on the specific requirements of the application [49].

The complementary filter can compensate for inherent errors in each sensor and provide a more reliable orientation estimate [40]. That is, the gyroscopes act as a low-pass filter to eliminate accelerometer noise, while the accelerometers

act as a high-pass filter to correct gyroscope drifts. Using this sensor-fusion approach, it is possible to obtain an accurate estimation of the human body's posture in space. This has practical applications in various fields [44].

Unscented Kalman Filter (UKF), an extension of the Kalman filter, is also used to fuse data from gyroscopes and accelerometers to estimate the orientation of the human body segments. This filter analyzes a series of observed measurements over time, including statistical noise and other uncertainties, to produce estimates of unknown variables that tend to be more accurate than those based on a single isolated measurement [50]. The UKF is capable of handling nonlinear systems [51] through a technique called the unscented transformation [52], [53] to estimate the state of the nonlinear system more accurately [54], [55], [56].

C. STUDY OBJECTIVES

This study aimed to quantify agricultural workers' exposure to ergonomic risks associated with their work posture. To achieve this, a UKF algorithm was developed to fuse accelerometer and gyroscope data to estimate the orientation of the sensors. This orientation was estimated in terms of quaternions as well as pitch and roll angles. Then a mathematical model was developed to use the output of the UKF to calculate human postural angles. This included trunk flexion-extension and lateral bending, upper arm flexion-extension and abduction-adduction, and elbow joint angles. Real-world data were collected from agricultural workers on site and was utilized in this calculation.

II. MATERIALS AND METHODS

A. DATA COLLECTION

Data were collected from a large plant nursery located 65 km from Montreal. Workers provided their informed consent to a human subject study of which the protocol was reviewed and approved by the Research Ethics Committee of the École de technologie supérieure (Reference H20211103, approved on January 21, 2022). Nine participants who worked in this facility were recruited; however, due to equipment malfunction during the data collection, data from only eight participants were used in this analysis. These participants had an average age of 38.5 (SD = 7.55) years, an average weight of 73.5 (SD = 4.78) kg, an average height of 1.65 (SD = 0.091) m and an average BMI of 25.93 (SD = 4.09). The participants were monitored by researchers from a distance where the researchers also took notes, photographs and videos.

B. TASKS

The participants' work day consisted of four sessions of varying duration from 1.75 to 2 hours. The last session was dedicated to the interview with the researchers as part of a larger study, so it was not included in this data analysis. Since the final goal of this study was to characterize postures separated by activity, sessions with similar work activities were grouped together. After reviewing the field notes, six distinct activity categories were identified as follows:

1) Supervision: 3 sessions, 1 participant
2) Mechanic Task: 6 sessions, 2 participants
3) Weeding: 6 sessions, 3 participants
4) Shrub Trimming: 1 session, 1 participant
5) Grass Sweeping: 1 session, 1 participant
6) Manual Plant Handling: 6 sessions, 3 participants

The full description of each activity, i.e., job task, is written in our qualitative paper about this study [57].

C. INSTRUMENTATION

This study used IMUs (SXT, Nexgen Ergonomics, Inc., Pointe Claire, Canada) to collect data for over 8 hours of the work shift. This was possible since the sensors were wireless and had a built-in memory that could ensure more than 8 hours of continuous recordings. In addition, it was not necessary to have a communication between the sensors and a computer during the recordings. This was perfect to the environment where the data were collected and the participants were far from one another. The IMU data were collected at its maximum sampling frequency of 128 Hz.

The IMUs were calibrated before the recording sessions using their proprietary software (TK Motion Manager, Nexgen Ergonomics, Inc., Pointe Claire, Canada). At this step, synchronous short static state sessions were recorded to set the IMUs' linear accelerations and angular velocities to zero, except that the vertical acceleration is set to equal to the gravitational acceleration.

On the data collection day, three IMUs were attached to the participants at their upper back between the two scapulae at the level of their superior angles, upper arm at the midpoint of the humerus on the lateral side, and forearm at the midpoint between the olecranon process and the styloid process of the ulna, as shown in Fig.1. The tracking at these three anatomical locations allowed the estimation of the inclination of the trunkas the angle measured away from the vertical line, the angle between the upper arm and the trunk, and the elbow angles.

All initial angles calculated from the accelerometers were filtered using a 4th order Butterworth low-pass filter with the cutoff frequency of 1 Hz [58].

D. DATA PROCESSING FOR SENSOR ORIENTATION ESTIMATION

The data processing of this study was divided into two primary steps: the estimation of sensor orientation and the calculation of posture. This section presents a customized UKF to combine accelerometer and gyroscope data, within Python 3.9.13. This UKF produced valuable orientation estimates in the form of Euler angles and quaternions.

The UKF algorithm consisted of three stages:

1) INITIALIZATION

The initialization of UKF involved obtaining the initial quaternion $\bar{x}_0$ from accelerometer data using (1) [59]. Here,

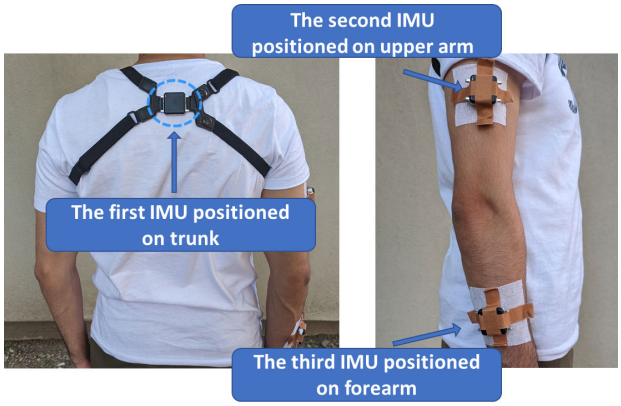

FIGURE 1. The positions of the IMUs on the three body segments.

600 stationary-state data points (approximately 5 seconds) were collected at the beginning of each session, and their median was used as the initial variable $\bar{x}_0$. The covariance matrix p_0^+ was initialized with small values as described in (2). Multiple p_0^+ values were tested, and the optimal one was selected [59].

$$\bar{x}_0 = \begin{cases} \left[\sqrt{\frac{a_z+1}{2}} \quad -\frac{a_y}{\sqrt{2(a_z+1)}} \quad \frac{a_x}{\sqrt{2(a_z+1)}} \quad 0\right]^T & \text{if } a_z \geq 0 \\ \left[-\frac{a_y}{\sqrt{2(1-a_z)}} \quad \sqrt{\frac{1-a_z}{2}} \quad 0 \quad -\frac{a_x}{\sqrt{2(1-a_z)}}\right]^T & \text{if } a_z < 0 \end{cases} \tag{1}$$

where a_x, a_y and a_z were the accelerations in the three directions: x as anteroposterior, y as media-lateral and z as vertical directions.

$$p_0^+ = 1 \times 10^{-3} \times I_{3\times 3} \tag{2}$$

2) PREDICTION

In the prediction step, gyroscope data $\omega_m = [\omega_x \ \omega_y \ \omega_z]$ was used to estimate the system state. This step involved several crucial sub-steps. Firstly, sigma points χ_k^i were computed from the previous state's covariance p_{k-1}^+ and estimated quaternions $\bar{x}_{k-1}$ based on (3) [50], [54], [56]. Secondly, new quaternions $\hat{x}_k^i$ were estimated via the function f from (4) and (5) [55], and then the predicted state's mean $\hat{x}_k$ was computed using (6). The third step involved computing the predicted state covariance p_k^- for all sigma points. This involved the addition of the covariance of the process noise Q_k, as shown in (7). The Q_k was computed using the predicted state's mean quaternions and the variance of three axes of the gyroscope $\sigma_{\omega_x}^2, \sigma_{\omega_x}^2, \sigma_{\omega_x}^2$ as shown in (8) [50]. Lastly, the prediction finished by deriving the new gyroscope bias b_k^+ using (9) [55].

$$\chi_k^i = \bar{x}_{k-1} \pm (\sqrt{L \cdot p_{k-1}^+})_i \quad \text{for } i = 1:2L \tag{3}$$

$$\hat{x}_k^i = f(\chi_k^i) \tag{4}$$

$$\hat{x}_k^i = \left(I_{4\times 4} + \frac{1}{2}\Delta t \Omega_m\right)\chi_k^i - \frac{1}{2}\Delta t [\triangleright]_q b_{k-1}^+ \tag{5}$$

$$\hat{x}_k = \frac{1}{2L}\sum_{i=1}^{2L} \hat{x}_k^i \tag{6}$$

$$p_k^- = \frac{1}{2L}\sum_{i=1}^{2L}\left(\hat{x}_k^i - \hat{x}_k\right)\left(\hat{x}_k^i - \hat{x}_k\right)^T + Q_k \tag{7}$$

$$Q_k = \frac{1}{4}\begin{bmatrix} -q_1 & -q_2 & -q_3 \\ q_0 & -q_3 & q_2 \\ q_3 & q_0 & -q_1 \\ -q_2 & q_1 & q_0 \end{bmatrix} \times \begin{bmatrix} \sigma_{\omega_x}^2 & 0 & 0 \\ 0 & \sigma_{\omega_y}^2 & 0 \\ 0 & 0 & \sigma_{\omega_z}^2 \end{bmatrix} \begin{bmatrix} -q_1 & -q_2 & -q_3 \\ q_0 & -q_3 & q_2 \\ q_3 & q_0 & -q_1 \\ -q_2 & q_1 & q_0 \end{bmatrix}^T \tag{8}$$

$$b_k^+ = b_{k-1}^+ + w_{b,k} \tag{9}$$

where:

L: Length of the state vector constituted by the four components of the quaternions, so L = 4

Δt: Time sample

ρ: The imaginary part of a quaternion

$w_{b,k}$: White noise of the gyroscopes

Ω_m was a 4 × 4 skew-symmetric matrix comprised of raw gyroscope measurement data ω_m, as shown in (10) [45].

$$\Omega_m = \begin{bmatrix} 0 & -\omega_m^T \\ \omega_m & -[\omega_m \times] \end{bmatrix} \tag{10}$$

The matrix $[v\times]$, where v represented a general variable, was a standard cross product matrix and defined in (11) [45].

$$[v\times] = \begin{bmatrix} 0 & -v_3 & v_2 \\ v_3 & 0 & -v_1 \\ -v_2 & v_1 & 0 \end{bmatrix} \tag{11}$$

The matrix $[\triangleright]_q$, which related the gyroscope noise vector $w_{b,k}$ and the gyroscope bias b_k^+, was given by (12) [45].

$$[\triangleright]_q = \begin{bmatrix} -\rho^T \\ q_0 I_{3\times 3} + [\rho\times] \end{bmatrix} \tag{12}$$

3) CORRECTION

To begin the correction step, new sigma points Φ_k^i were computed from the predicted state mean $\hat{x}_k$ and the covariance p_k^-, as shown in (13) [50], [54], [56]. Then, predicted measurements $\hat{y}_k^i$ in the form of the pitch and roll angles, were generated for each sigma point using the measurement function H in (14) and (15) [45], [50], [60]. Next, their mean yielded the predicted measurement mean $\hat{y}_k$ as shown in (16). Also, the predicted measurement covariance p_k^y was computed using (17), which involved adding the covariance of the measurement noise R_k [50]. The covariance between the prediction and the correction p_k^{xy} was determined by (18), leading to the calculation of the gain matrix K_k in (19). This gain matrix was then employed to estimate the actual state $\bar{x}_k$ by utilizing the difference between the actual measurement $y_{\text{real},k}$ and the predicted measurement mean $\hat{y}_k$ as illustrated in (20). Finally, the corrected state covariance p_k^+ was computed using the gain matrix K_k, the predicted state

covariance p_k^- and the predicted measurement covariance p_k^y according to (21). This adjusted covariance was used in the subsequent iteration of the UKF.

$$\Phi_k^i = \hat{x}_k \pm (\sqrt{L \cdot p_k^-})_i \quad \text{for } i = 1:2L \tag{13}$$

$$\hat{y}_k^i = \mathcal{H}(\Phi_k^i) = \begin{bmatrix} \theta(\Phi_k^i) \\ \phi(\Phi_k^i)] \end{bmatrix} \tag{14}$$

$$\hat{y}_k^i = \begin{bmatrix} \text{atan2}\left(\frac{2(q_0q_2 - q_1q_3)}{q_0^2 - q_1^2 - q_2^2 + q_3^2}\right) \\ \text{atan2}\left(\frac{2(q_0q_1 + q_2q_3)}{q_0^2 - q_1^2 - q_2^2 + q_3^2}\right) \end{bmatrix} \tag{15}$$

$$\hat{y}_k = \frac{1}{2L}\sum_{i=1}^{2L} \hat{y}_k^i \tag{16}$$

$$p_k^y = \frac{1}{2L}\sum_{i=1}^{2L} (\hat{y}_k^i - \hat{y}_k)(\hat{y}_k^i - \hat{y}_k)^T + R_k \tag{17}$$

$$p_k^{xy} = \frac{1}{2L}\sum_{i=1}^{2L} (x_k^i - x_k)(\hat{y}_k^i - \hat{y}_k)^T \tag{18}$$

$$K_k = p_k^{xy} \cdot (p_k^y)^{-1} \tag{19}$$

$$\bar{x}_k = \hat{x}_k + K_k \cdot (y_{\text{real},k} - \hat{y}_k) \tag{20}$$

$$p_k^+ = p_k^- - K_k \cdot p_k^y \cdot K_k^T \tag{21}$$

where the covariance of the measurement noise R_k was the dot product of the matrix M and the variance of the accelerometer along the three axes $\sigma_{a_x}^2$, $\sigma_{a_y}^2$ and $\sigma_{a_z}^2$ (22) [50].

$$R_k = M \cdot \text{div}_{\text{accel}} \cdot M^T \tag{22}$$

with:

$$M = \begin{bmatrix} 0 & \frac{a_z}{a_y^2 + a_z^2} & -\frac{a_y}{a_y^2 + a_z^2} \\ -\frac{\sqrt{a_y^2 + a_z^2}}{a_x^2 + a_y^2 + a_z^2} & \frac{a_x a_y}{(a_x^2 + a_y^2 + a_z^2)\sqrt{a_y^2 + a_z^2}} & \frac{a_x a_z}{(a_x^2 + a_y^2 + a_z^2)\sqrt{a_y^2 + a_z^2}} \end{bmatrix} \tag{23}$$

The $y_{\text{real},k}$ was the transformation of accelerometer data a_x, a_y, a_z to pitch and roll in Euler angles using trigonometry (23) [61].

E. DATA PROCESSING FOR POSTURE ESTIMATION

Transitioning to the second step, this section is dedicated to the posture estimation. The comprehensive plan is outlined in Fig.2, Fig.3 and Fig.4.

Overall, this stage involved a calibration procedure that achieved orientation alignment within the coordinates of individual body segments for each sensor. Also, to further improve the estimation of elbow angle, the impact of the movements of the upper arm relative to the trunk was taken into account through the quaternion's conjugation operation.

1) SENSOR ALIGNMENT

The reason for transforming the sensor data on a global coordinate system to body segment coordinates was to study the orientation of the trunk and the angles of upper extremities. That is, each body segment, namely the trunk, upper arm, and forearm, had its own local coordinate system. This technique was useful since the interest of this study was to analyze the postures of the body segment where the IMUs are attached [62].

From the IMUs, the accelerations and angular velocities were initially in the global coordinate system. The UKF was applied on these accelerations and angular velocities to determine the orientation of the IMU sensor at each time step relative to the initial orientation as shown in the part 1 of Fig.2.

After the UKF yielded angles in the global coordinate, the subsequent step involved computing angles of trunk, upper arm and forearm. At the start of the recording session, participants stayed in a static position, where all their segments were aligned vertically while data were captured as a baseline. This process is referred to as *Ipose*. This recording lasted about 4 to 5 seconds. Subsequently, this data was fed into the UKF. For each *Ipose*, three parameters were acquired: the two Euler angles (θ_{IPose}, ϕ_{IPose}) and the quaternions ($q_{0,Ipose}$, $q_{1,Ipose}$, $q_{2,Ipose}$, $q_{3,Ipose}$), as presented in the part 2 of Fig.2.

The quaternion of the *Ipose* was considered as the orientation of the body segment in the global reference and used to transform the quaternion estimated by the UKF into the initial orientation of trunk, upper arm or forearm, which was still in the global coordinate through a quaternion multiplication. The following steps were followed:

1) The conjugation of the median quaternion from the *Ipose* (24),
2) The multiplication of the conjugated quaternion with the quaternion estimates, obtained from the UKF, to derive rotational quaternion estimates in the body coordinate reference (25).

$$\text{conj}(q_{\text{IPose}}) = [q_{0,\text{Ipose}} \ -q_{1,\text{Ipose}} \ -q_{2,\text{Ipose}} \ -q_{3,\text{Ipose}}] \tag{24}$$

$$q_{\text{body}} = q_{\text{global}} \cdot \text{conj}(q_{\text{IPose}}) \tag{25}$$

In Euler angle, the *Ipose* angles (θ_{IPose}, ϕ_{IPose}) were subtracted from the UKF-calculated pitch and roll angles (θ and ϕ) to obtain calibrated angles in the local coordinates of each specific segment ($\theta_{\text{calibrated}}$, $\phi_{\text{calibrated}}$) [63]. The final Euler angles were calculated using (26) and (27). This subtraction of two Euler angles had already been validated and used in previous studies [63], [64].

$$\theta_{\text{calibrated}} = \theta - \theta_{\text{IPose}} \tag{26}$$

$$\phi_{\text{calibrated}} = \phi - \phi_{\text{IPose}} \tag{27}$$

Given the study's emphasis on the trunk, upper arm and forearm segments, the previously-described process was applied to each of the three segments. This yielded calibrated quaternions (q_{Trunk}, $q_{Upperarm}$, $q_{Forearm}$) and Euler angle values, as shown in the part 3 of Fig.2.

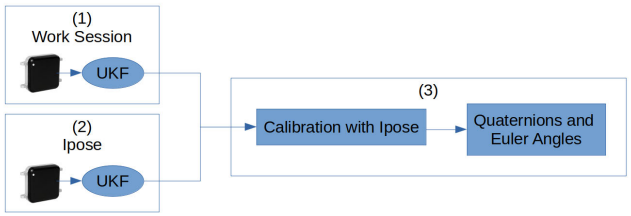

FIGURE 2. The transformation of sensor data from sensor coordinates to body coordinates, part 1 estimating orientation in sensor coordinates using UKF, part 2 estimating orientation of the Ipose, and part 3 aligning orientation in sensor coordinates to body coordinates using the Ipose.

From the schema in Fig.2, the trunk inclination was directly calculated.

2) SHOULDER AND ELBOW ANGLES CALCULATION

Unlike the calculation of trunk inclination, in which only one sensor was used, the shoulder and elbow angles accounted for multiple segments. That is, the shoulder angle was the angle between the trunk and the upper arm, and the elbow angle was one between the upper arm and the forearm.

In Euler angles, the calibrated upper arm angles were directly subtracted from the calibrated trunk angles, as mentioned in (28) and (29). This direct subtraction technique had also been validated and used in previous studies [63], [64]. However, in quaternions, the angles were obtained by performing a quaternion multiplication between the calibrated upper arm quaternions and the conjugate of the calibrated trunk quaternions (30). The whole process for the upper arm angle calculation is shown in Fig.3.

$$\theta_{\text{calibrated Upperarm}} = \theta_{\text{Upperarm}} - \theta_{\text{trunk}} \tag{28}$$

$$\phi_{\text{calibrated Upperarm}} = \phi_{\text{Upperarm}} - \phi_{\text{trunk}} \tag{29}$$

$$q_{\text{calibrated Upperarm}} = q_{\text{Upperarm}} \times \text{conj}(q_{\text{trunk}}) \tag{30}$$

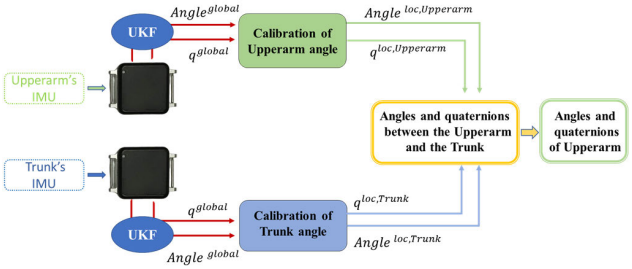

FIGURE 3. The characterization of upper arm's posture.

To calculate the elbow angle, it was necessary to subtract the rotation of the forearm from the total rotation of the upper arm. This operation was achieved by multiplying the corresponding quaternions of the upper arm q_{Upperarm} by the conjugated quaternions of the forearm $q_{Forearm}$ as shown in (31) [65].

$$q_{\text{Elbow}} = q_{\text{Upperarm}} \times \text{conj}(q_{Frearm}) \tag{31}$$

As presented in Fig.4, the elbow angle calculation accounted for upper arm movement relative to the reference, which was the trunk. That is, a quaternion multiplication was performed on the previously-calibrated elbow quaternion q_{Elbow} and the conjugate of the trunk quaternion q_{Trunk}, as described in (32) [66].

$$q_{\text{Calibrated, Elbow}} = q_{\text{Elbow}} \times \text{conj}(q_{\text{Trunk}}) \tag{32}$$

Then the elbow angle in radian ρ was obtained from the previously-calculated quaternion $q_{\text{Calibrated, Elbow}}$ through (33) [66].

$$\rho = \text{Atan2}\left(\frac{1-(q_2^2+q_3^2)}{2(q_0q_3+q_1q_2)}\right) \tag{33}$$

Finally, all the angles of interest (i.e., trunk flexion-extension and lateral bending, upper arm flexion-extension and abduction-adduction, and elbow flexion) in the time series of each session were summarized in terms of the 10th, 50th and 90th percentiles, and the percentages of work time spent on the ranges of angles used in the standard ergonomic evaluation [14], [15]. Across multiple sessions, the medians and interquartile ranges of the percentiles of the three joint angles and the percentages of time when workers were exposed to specific postures were then calculated.

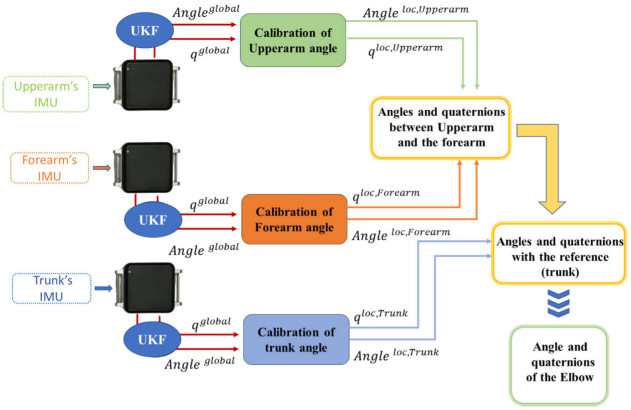

FIGURE 4. The characterization of elbow angle.

III. RESULTS

The results are presented in two main parts: first, the validation of the newly-developed UKF and, second, the calculated postures and postural exposures during each work activity.

A. VALIDATION OF THE UNSCENTED KALMAN FILTER

1) VALIDATION WITH A GONIOMETER

A preliminary validation for the UKF was conducted using a goniometer at stationary states. After every 5 seconds, constant increments of 10° was introduced until all the 360° was covered. The findings demonstrated that the UKF performed well, exhibiting congruent results with the goniometer. In particular, the computed RMSE values for the pitch and roll angles were 0.0298° and 0.0408°, respectively. This showed the UKF's remarkable accuracy in static conditions.

2) VALIDATION WITH KALMAN FILTER

The second validation was conducted on the real data under dynamic conditions. That is, a 300-second chunk of the data collected in the field was used. This data was collected while participants were wearing the IMUs and performing their regular work tasks. The results from UKF were compared with ones applying the Kalman filter developed by Chen et al. [40]. As shown in Fig.5 and Fig.6, during a 5-minute section of the weeding task, the UKF produced approximately similar roll and pitch estimates, while being noticeably smoother and more stable than the Kalman filter. Additionally, this visualization of similarity was supported by the low RMSE values of 0.78° and 1.28° for the roll and pitch angles, respectively. Furthermore, while the Kalman filter cannot estimate pitch angles beyond ±90° due to its mathematical model [40], the UKF developed in this study overcame this limitation.

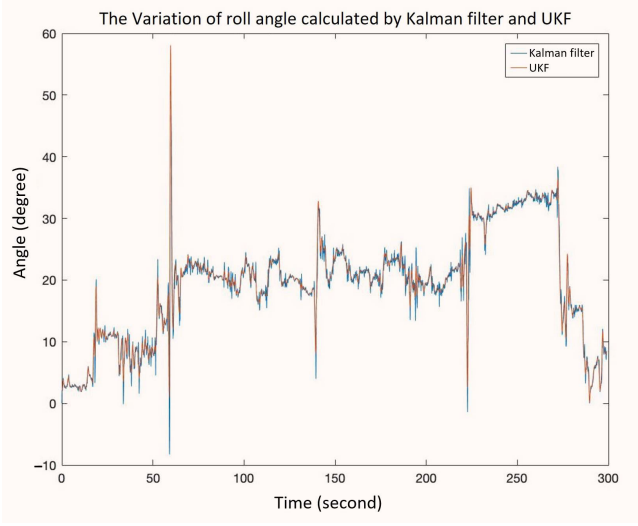

FIGURE 5. The variation of roll angle over time from Kalman filter and UKF.

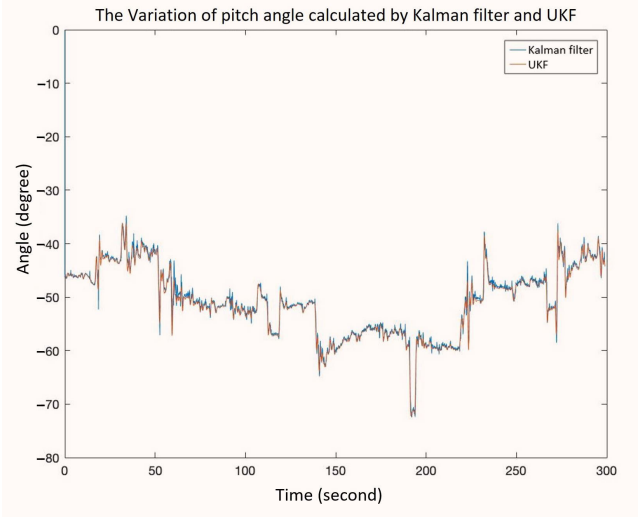

FIGURE 6. The variation of pitch angle over time from Kalman filter and UKF.

3) VALIDATION WITH MOTION CAPTURE SYSTEM

Finally, the validation for dynamic performance was also conducted by comparing the results from our UKF algorithm as compared to the angles estimated from the Motion Capture System (MoCap). The data lasts approximately over one minute. The sampling rate for the MoCap was 120 Hz. As the IMU's sampling rate was 128 Hz, we had to downsample the IMU data prior to calculate the RMSE as compared to the MoCap. Then, instead of roll or pitch angle, we directly compared the quaternions and found the average RMSE of 11.42°.

B. WORK POSTURES

The outcomes of the six activities are shown in Tables 1 and 2.

1) ACTIVITY 1: SUPERVISION

In the supervision task, while trunk extension was almost negligible (0.03% of the work time), the worker's exposure to trunk flexion was high with 82.96% within the 20°-to-60° range of flexion. This insignificant extension was also confirmed by the 10th percentile of the flexion-extension angle at 18.67°. Lateral bending was mainly in the 0°-to-20° range (82.84%), followed by 14.15% within the range between 20° and 60°, while only 3% of the time exceeding 60°. This was reflected by the median of only 13.49° and the 90th percentile as small as 25.32°.

Upper arm flexion was predominant, with 12.59% of the time in the 20°-to-45° range and 81.43% in the 45°-to-90° range. Meanwhile, upper arm extension exposure was less than 5% of the work time. In terms of arm abduction-adduction, the abduction was accounted for about 87% of the work time, leaving the adduction exposure to be approximately only 17%.

The elbow angles were mostly within the range from 0° to 90° (50.97%), with the median angle of 84.86°. Also, there existed smaller portions of elbow angles in the ranges from 90° to 120° (12.46%) and from 120° to 160° (25.81%), while angles above 160° accounted for 10.76%.

2) ACTIVITY 2: MECHANICS

During the activities performed by the two mechanics, slight trunk extension was observed at 8.53% of the total time. The time spent with trunk flexion was 26.38% in the range from 0° to 20°, 47.94% in the range from 20° to 60°, and 10.83% of angles was greater than 60°. The presence of the flexion was clearer than the extension, which was also indicated by the 10th percentile of 0.89° and the median of 32.7°. For the lateral bending exposure, 78.71% of the work time was in the 0°-to-20° angle range, 12.51% was in the 20°-to-60° range, and 8.79% was in the angles exceeding 60°. The median angle of the lateral bending was considered fairly small (10.58°). However, the extreme or the 90th percentile lateral bending was as high as 52.98°. Still, since its IQR among the six sessions was fairly large (55.1°), this implied the high diversity of postures in this mechanics activity.

TABLE 1. Angles in degrees in the percentile ranks for the different postures in the six activities:Mean(SD). Note that N/A's in the mean field are missing values, and N/A's in the SD are from the sample size of one.

Angle	Percentile	Activity 1	Activity 2	Activity 3	Activity 4	Activity 5	Activity 6
Trunk							
Flexion-Extension	10th	18.67 (11.58)	0.89 (14.84)	13.51 (6.39)	N/A	N/A	18.3 (3.57)
	50th	26.25 (10.37)	26.38 (9.47)	40.46 (5.07)	N/A	N/A	28.56 (4.73)
	90th	42.50 (7.77)	61.90 (32.21)	124.41 (6.61)	N/A	N/A	52.99 (16.63)
Lateral bending	10th	5.69 (1.53)	1.92 (0.46)	6.94 (0.91)	N/A	N/A	3.20 (1.56)
	50th	13.49 (1.82)	10.58 (3.87)	27.88 (2.36)	N/A	N/A	13.02 (4.03)
	90th	25.32 (4.91)	52.98 (55.1)	138.42 (6.66)	N/A	N/A	44.67 (18.94)
Upper Arm							
Flexion-Extension	10th	42.33 (22.5)	27.35 (23.46)	-48.63 (38.31)	-17.0 (N/A)	-7.0 (N/A)	-0.84 (62.0)
	50th	58.14 (2.08)	51.52 (15.88)	3.16 (4.17)	0.0 (N/A)	27.0 (N/A)	24.62 (43.9)
	90th	73.63 (3.95)	85.89 (22.65)	54.74 (23.2)	50.0 (N/A)	71.0 (N/A)	62.76 (35.87)
Upper Arm							
Abduction-Adduction	10th	-4.52 (23.72)	-51.31 (36.17)	-26.99 (38.74)	-25.0 (N/A)	-44.0 (N/A)	-67.50 (33.61)
	50th	15.90 (2.27)	-4.70 (6.54)	7.63 (14.95)	3.0 (N/A)	20.0 (N/A)	-8.54 (7.98)
	90th	36.88 (6.63)	36.16 (34.11)	65.07 (19.96)	26.0 (N/A)	63.0 (N/A)	27.84 (14.39)
Elbow							
Flexion-Extension	10th	18.86 (17.67)	20.09 (3.67)	20.48 (1.5)	22.0 (N/A)	21.0 (N/A)	21.08 (2.64)
	50th	84.86 (22.95)	88.23 (7.3)	87.76 (3.42)	88.0 (N/A)	82.0 (N/A)	88.11 (6.47)
	90th	161.67 (2.27)	158.38 (2.78)	158.55 (1.21)	156.0 (N/A)	155.0 (N/A)	162.28 (4.98)

TABLE 2. Percentage of time in the total work time taken by each posture in the six activities: Mean(SD). Note that N/A's in the mean field are missing values, and N/A's in the SD are from the sample size of one.

Angle	Range	Activity 1	Activity 2	Activity 3	Activity 4	Activity 5	Activity 6
Trunk Extension	< 0	0.03 (1.08)	8.53 (6.64)	1.78 (1.25)	N/A	N/A	1.08 (49.98)
Trunk Flexion	0 to 20	13.62 (26.00)	32.70 (29.96)	14.76 (5.07)	N/A	N/A	3.57 (7.04)
	20 to 60	82.96 (25.74)	47.94 (9.14)	41.73 (8.02)	N/A	N/A	84.83 (2.45)
	> 60	3.39 (1.76)	10.83 (6.16)	41.74 (1.69)	N/A	N/A	10.51 (3.41)
Lateral bending	0 to 20	82.84 (8.09)	78.71 (15.37)	42.68 (2.19)	N/A	N/A	67.60 (7.34)
	20 to 60	14.15 (7.66)	12.51 (4.22)	15.40 (0.40)	N/A	N/A	24.27 (7.25)
	> 60	3.01 (1.55)	8.79 (7.85)	41.92 (1.79)	N/A	N/A	8.13 (2.96)
Upper Arm Flexion	0 to 20	0.03 (3.47)	3.03 (7.69)	21.41 (16.52)	32.99 (N/A)	23.71 (N/A)	28.62 (22.36)
	20 to 45	12.59 (11.66)	33.84 (10.27)	13.93 (6.08)	5.15 (N/A)	36.08 (N/A)	23.65 (12.16)
	45 to 90	81.43 (20.10)	53.69 (16.34)	12.93 (14.73)	11.34 (N/A)	20.62 (N/A)	29.86 (51.04)
	> 90	1.81 (0.64)	8.56 (4.12)	1.76 (0.24)	0 (N/A)	4.12 (N/A)	3.69 (5.49)
Upper Arm Extension	0 to -20	4.05 (11.55)	0.17 (4.20)	21.04 (0.42)	43.30 (N/A)	11.34 (N/A)	11.89 (1.05)
	< -20	0.09 (0.14)	0.71 (2.53)	28.94 (0.03)	7.22 (N/A)	4.12 (N/A)	2.30 (22.12)
Upper Arm Abduction	0 to 20	46.07 (9.19)	27.03 (16.49)	25.27 (20.87)	45.92 (N/A)	22.22 (N/A)	19.69 (1.11)
	> 20	37.03 (4.62)	16.63 (3.64)	44.9 (18.58)	15.31 (N/A)	50.51 (N/A)	16.15 (10.21)
Upper Arm Adduction	0 to -20	13.07 (3.07)	29.53 (11.20)	16.85 (5.87)	26.53 (N/A)	11.11 (N/A)	27.54 (19.72)
	< -20	3.84 (8.54)	26.81 (6.30)	12.98 (24.90)	12.24 (N/A)	16.16 (N/A)	36.62 (13.29)
Elbow							
Flexion-Extension	0 to 90	50.97 (12.52)	50.72 (3.31)	50.53 (1.61)	51.02 (N/A)	54.08 (N/A)	49.44 (2.97)
	90 to 120	12.46 (3.92)	14.43 (2.07)	13.85 (2.11)	14.29 (N/A)	14.29 (N/A)	14.32 (1.11)
	120 to 160	25.81 (6.83)	25.90 (3.49)	26.74 (1.03)	27.55 (N/A)	24.49 (N/A)	24.59 (0.81)
	> 160	10.76 (3.38)	8.95 (1.65)	8.88 (0.67)	7.14 (N/A)	7.14 (N/A)	11.66 (4.10)

The upper arm movement was dominated by the flexion, with 33.84% of the work time having upper arm flexion in the 20°-to-45° range, 53.69% in the 45°-to-90° range, and 8.56% above 90°. Upper arm extension was, in contrast, negligible (less than 1%) and the 10th percentile of the upper arm flexion-extension was 27.35°. The time spent with upper arm abduction and time with adduction were somewhat equal and its median angle was $-4.7°$. Nevertheless, it should be noted that the adduction prevailed beyond 20° for 26.81%. This was possible at the time when the participants lied down and raised their arms over their body to fix something under the machine.

Regarding the elbow angles, the participants spent 50.72% of the time having their elbow angle within the 0°-to-90° range. In the other ranges of interest, the angles were from 90° to 120° for 14.43%, from 120° to 160° for 25.90%, and above 160° for 8.95%.

3) ACTIVITY 3: WEEDING

While weeding, the participants were exposed to remarkable trunk flexion. That is, the workers spent a great amount of time (greater than 80%) in their stooping position, i.e., 20° to 60° for 41.73%, and greater than 60° for 41.74%. Moreover, the median trunk flexion was 40.46° and the high-intensity flexion or its 90th percentile was as high as 124.41°. Lateral bending also stood out. On one hand, the lateral bending was mainly closer to the neutral range in the 0° to 20° (42.68%), which was likely when the worker were standing. On the

other hand, the greater angles above 60° were also observed for 41.92% of the time, which could be the time when the workers stooped over to pick up the weed.

For the upper arm movements, both flexion and extension were generally neutral. They occurred primarily in the 0° to 20° range (21.41% for extension and 21.04% for flexion). Nonetheless, larger angles used in the extension posture also occurred (28.94%). The abduction were more predominant than the adduction (70% v.s. 30%, respectively).

In terms of elbow angle, the range from 0° to 90° were the most common (50.53%), while the angles extended beyond 160° were found the rarest (8.88%).

4) ACTIVITY 4: SHRUB TRIMMING

The shrub trimming activity consisted of fairly neutral upper arm movements. The flexion-extension angles simply had the median of 0°. The most common ranges for both flexion and extension posture were within the 0°-to-20° range (about one-third of the work time), with 32.99% of the time spent on this slight flexion and 43.3% of the time spent on small extension. The abduction-adduction angles were also marginal, with two-third of the time spent in the neutral range (0° to −20°). Slight abduction was the most common (45.92%) as compared to the other ranges.

Elbow angles were predominant within the range from 0° to 90° (51.02%), which seemed to be representative to the shrub trimming activity when the participants operated the garden shear.

5) ACTIVITY 5: GRASS SWEEPING

In grass sweeping activity, upper arm flexion was moderate. On one hand, the time in the neutral range from 0° to 20° was 23.71%. On the other hand, the angle ranges from 20° to 45° and those from 45° to 90° were also somewhat frequent, accounting for 36.08% and 20.62%, respectively. In contrast, upper arm extension was quite small (about only 15% of the total time). The abduction above 20° was present with the high percentage of work time (50.51%) as compared to others; however, the time spent with arm adduction posture, i.e., angles smaller than −20° were quite little (16.16%). Regarding the elbow angles, the range from 0° to 90° was the most common (54.08%) in this grass sweeping activity.

6) ACTIVITY 6: MANUAL PLANT HANDLING

This activity refers to the time when the participants loaded the plant containers to the truck and unloaded them to the shipping area. While performing this activity, the participants had trunk flexion primarily in the 20°-to-60° range (84.83%) but had minimal trunk extension (1.08%). The lateral bending was observed mostly in the 0°-to-20° range (67.6%), followed by the 20°-to-60° range (24.27%).

The flexion of the upper arm occurred more frequently than the extension (about 85% v.s. 15%). This upper arm flexion could be considered very important since the 90th percentile of the angle was 62.76° and the median angle was 24.62°. The abduction and adduction of the arms exhibited in a large range (from −67.5° to 27.84° as shown in the 10th and 90th percentiles of the angle). In the majority of the work time, the participant had non-neutral abduction-adduction postures, i.e., having their arm abducted for more than 20° for 16.15% of their time and working in the arm adduction posture for 36.62% of the time.

The elbow angles were less than 90° for a significant amount of time (49.44%). This corresponded with the median of the elbow angle at 88.11°. The general range of motion was presented with the 10th and 90th percentiles of 21.08° and 162.28°, respectively. It is worth noting that the manual plant handling exhibited some elbow extension; that is, the elbow angle was above 160° for 11.66% of the work time. This was probably the time when the participants had to stretch their arms to carry the plant containers on each side of their body.

IV. DISCUSSION

A. UNSCENTED KALMAN FILTER

In this research, a new UKF was developed to fuse the IMU's accelerometer and gyroscope data to estimate the orientation of human body segments. The validation at static state with an analog goniometer, with the angle raging from -2π to 2π and with the increment of 10°, showed marginal RMSE suggesting that the UKF successfully estimated the angles from the IMU as compared to the goniometer. Additionally, a comparison between the UKF approach and the Kalman filter developed by Chen et al. [40] showed promising results, with the RMSE of 1.28° and 0.78° for pitch and roll, respectively, demonstrating accuracy and stability of the UKF. This confirmed the prior knowledge that the UKF would handle non-linearity and non-Gaussian noise typically presented in the signals of human body movements. The study's findings emphasized the UKF's advantages in providing stable estimates, especially in dynamic movements with large variation, highlighting its potential for applications in estimating human body posture from IMU data. Even though the RMSE as compared to the gold-standard MoCap during a continuous movement remains moderate (11.42°), this amount of error may be considered acceptable for the purpose of posture estimation in the ergonomic context.

Furthermore, regarding the 3D rotation, quaternions was chosen as the preferred method due to their reliability and rigidity. Quaternions provided a compact representation of 3D rotations and were less prone to encountering singularity issues compared to other rotation methods. The use of quaternions in this study ensured a more robust and stable estimation of postures [45], [67], [68].

Besides, the UKF initialization was crucial for posture estimation, considering parameters like the state vector and covariance matrix. On one hand, simple zero-initialized state vectors could have led to slow convergence [65]. On the other hand, more complex methods like the quaternion factorization algorithm would be effective but computationally demanding [69]. In this study, the state vector in quaternions was initialized using accelerometer data [59], proving its

effectiveness with less complexity. In addition, the covariance matrix, usually positive definite, with high values, could have caused noisy estimates [70]. Meanwhile, in this study, it was initialized with small values (10e3), affecting only the initial estimation stage.

B. IMPROVED METHOD FOR ESTIMATING POSTURE

Unlike laboratory-based studies using a motion capture system such that the global coordinate can be directly set [71], [72], [73], field-base studies using IMUs would require a reference, that would also needed to be measured. In this study, a simple and effective method for measuring a reference coordinate and calibrating for angles was adopted [63]. The reference posture, or Ipose, was when a subject stood with back straight and arms hanging down. This Ipose measurement represented the local segment orientations in the global coordinates. Then the calibration involved subtracting the estimated local segment angles from the median angles of the Ipose phase. This subtraction corrected angle estimations in local segment coordinates. By using the median angles from the Ipose phase, the reference orientations were not subjected to variations that might have been due to unintentionally non-stationary situation.

While previous studies estimated postures based on individual body segment coordinates, neglecting interactions and dependencies between body parts [63], this study took a different approach, using the trunk as a reference for other body parts. The consideration of the trunk movement in this study significantly influenced the upper arm posture's estimation, leading to more accurate results, especially in situations or activities that greater trunk flexion or lateral bending was frequent. Moreover, the angles of the elbow were also estimated, considering the movement of the upper arm relative to the trunk. By accounting for the inter-segment relationships, we employed the approach to improve the accuracy of the estimation, as proven by the previous study [65].

In conclusion, it should be noted that few studies have comprehensively evaluated various upper body postures. This gap may be due to mathematical modeling complexities or methodological limitations. Our study provided a comprehensive and holistic view of upper body postures, considering the interplay between different body segments from trunk, upper arm and forearm. This is considered a significant contribution to the ergonomics discipline.

C. COMPARISON WITH PREVIOUS STUDIES

1) COMPARISON BASED ON WORK ACTIVITIES

Our findings presented some similarities with previous studies [74], [75], [76] on certain activities. Based on the actual movement that the participants performed on the data collection day, our supervision task (Activity 1) could be considered as ''manual work'' or ''mixed between driving and manual work'' as explored by Fethke et al. [75]. Comparing between the two studies, the supervisor in our study exhibited slightly more back flexion than those in [75]. Yet, in both studies, extreme trunk flexion were minimal, accounting for less than 4% of the total task time. Although the lateral bending found in both studies stayed within a neutral range of $\pm 20°$, with over 80% of the work time for each group, the maximal lateral bending was higher among our supervision task than one in the previous study. This was likely due to the fact that the supervisor at this plant nursery often went out of his way to help the other workers in manual tasks such as planting (not recorded in this study), which involved a greater degree of lateral bending.

Moreover, the equipment repair/maintenance in the study by Fethke et al. [75] corresponded to the mechanics activity in our study (Activity 2). It was observed that workers in our study adopt extreme back or trunk flexion posture with higher degrees. That is, the 90th percentile reached 61.9°, while in the study by Fethke et al. the 90th percentile was only 46.6°. Additionally, between the two studies, the more pronounced difference was observed in the lateral bending. That is, Fethke et al. found extreme values of $-14°$ for the left side and 14.7° for the right side [75]. In contrast, in our study, the 90th percentile reached 52.98°, exceeding the threshold considered dangerous for this posture, set at 30° [76].

Furthermore, a previous study by Granzow et al. [76] provided a highly comparable situation with 14 seasonal workers dedicating 75.8% of work time to manual reforestation, called ''gardening''. This population was also similar to our study in terms of demographics and anthropometry. From the work posture perspective, this activity was considered similar to our weeding activity (Activity 3). The extreme back flexion during weeding exhibited very high intensity, with the 90th percentile of 124.41°, whereas in the gardening activity, the 90th percentile was 80.2° [76]. While gardeners adopted moderate lateral bending, ranging from $-14.3°$ on the left side to 9.4° on the right side, our weeding activity exposed the workers to more extreme postures, with the 90th percentile as high as 138.42°. Regarding the upper arm flexion, it was found more frequent in the gardening activity than the weeding. Overall, both activities presented a significant number of potentially hazardous postures, but weeding was characterized by the greater frequency of high-intensity postures for the back.

In addition, in the study by Granzow et al. [76], the remaining time was allocated to non-planting activities, such as loading sacks, shaking and tapping seedlings against objects to remove particles, unloading and transporting seedling boxes to vehicle-inaccessible gathering areas [76]. These activities corresponded to the manual plant handling activity in our study (Activity 6). On one hand, this non-planting activity featured a slightly lower median of back flexion than ours (20.4° v.s. 28.6°). On the other hand, their study showed somewhat greater high-intensity back flexion in non-planting activities than ours, with the 90th percentile of 57° as compared to ours at 53°. Still, such differences could be considered marginal or practically insignificant. As for the lateral bending, the non-planting activity maintained a neutral

position with an range of ±9°, while manual plant handling exhibited a larger lateral bending. Manual plant handling was considerably higher in the Manual Plant Handling activity.

Finally, for the two remaining activities, namely shrub trimming and grass sweeping (Activities 4 and 5), no other activity with a similar profile was identified in the existing literature. However, in general, these activities were characterized by moderate back postures. The movements of upper arm flexion, adduction and abduction could be observed with extreme intensities.

2) OVERALL COMPARISON WITH DIFFERENT INDUSTRIES

Our study can be compared to previous studies in other industries as well as those in other agricultural commodities.

First, our research was different from the study conducted by Lee et al. [77], which was focused on assessing trunk angles during janitorial work identified as fast-paced and physically intense and often resulting in unfavorable posture. While Lee et al. observed that 50th percentile for trunk angles were approximately 15°, our study recorded a notably higher angle of 26.38°. This indicates that plant nursery activities generally require more trunk flexion postures. Furthermore, when considering the percentage of time that individuals spent in postures ranging from 20° to 60°, Lee et al. found that the maximum duration was around 32%. In our study, however, the minimum duration for these postures was 41.73%, and, in some cases, it rose to as high as 84.83%. This demonstrates a substantial difference in the duration of these postures between the two studies. When comparing extreme trunk postures, specifically those exceeding 60°, Lee et al. showed relatively low occurrences, with an average of around 3% of the work time, except for the restroom cleaning, which had the highest percentage at about 7% of the time. These percentages seemed notably smaller when compared to our results, where the range of postures above 60° occupied as much as 41.47% of the time for weeding activity.

Second, our study was also compared to a study in the horticultural industry Thamsuwan et al. [64] relevant to upper arm flexion. On one hand, for the 50th percentile of upper arm flexion angles in the aforementioned study, the results within a range of 18° to 26° was quite similar to our study in the case of our sweeping and manual material handling, but not for the tasks performed by the supervisors and mechanics in our study. On the other hand, for the extreme posture like the 90th percentile of upper arm flexion, our study (50°−86°) indicated more substantial values than those found in the compared study (43°−55°). Regarding the upper arm abduction, the results from both studies are relatively close to each other for both the 50th and 90th percentiles.

D. LIMITATIONS AND RECOMMENDATIONS

The UKF algorithm had an inherent complexity and high computational demand, leading to long execution time. This was primarily driven by the process of regenerating sigma points and applying them to the nonlinear state and the measurement function at each time step. Memory usage became a substantial concern in storing and manipulating sigma points, especially in the case of extended duration sessions of data collection, like those encountered in this study (2 hours).

Another shortcoming of the UKF developed in this study is that the initialization of the parameters was simplified. Instead, optimizing the input parameters of the UKF, including the state vector and the covariance matrix, and using various weights in formulating sigma points, might improve the UKF's accuracy [65], [70], [78]. Further work regarding these parameters using the methods elaborated upon in the discussion section, the ''unscented Kalman filter'' subsection, has a potential to enhance the outcomes of the UKF.

Once the UKF parameters are optimized and the algorithm is validated, a comparative analysis between the use of these IMU sensors and a motion capture system can be done. The use of such a gold standard method for validation is expected to improve even more the accuracy of the posture estimation.

Furthermore, one practical aspect of our study leading to future work would be to apply our posture estimation algorithm to data collected from less robust sensors like smartphone's IMUs. For instance, a study by Nath et al. [79] used accelerations from smartphones to calculate trunk inclination and upper arm angles to identify ergonomic risks in gross levels. They also mentioned the possible use of angular velocities. Their idea of using sensors already available for everyone who has a smartphone could make such research affordable and extendable to a larger scale. Meanwhile, they could predict simply the level of risk that may not be precise. To compliment this idea, our work employing UKF may be integrated into this prediction.

Finally, the outcomes of this research will be used as input for a new analysis using machine learning technique with the objective to re-group work sessions into activities with similar postures and postural exposures such that similar intervention may be applied.

V. CONCLUSION

This study provided a new method for posture estimation using IMUs and their application for ergonomic risk assessment among agricultural workers. The initial challenge was the high magnetic radiation noise in the data collection environment. To address this problem, a novel sensor-fusion filter, the UKF algorithm, was developed to integrate accelerometer and gyroscope measurements for optimal posture estimation. The UKF exhibited substantial advantages. First and foremost, the trunk flexion or forward bending estimated from pitch angles could be extended to a wider range (up to 180°) as compared to the Euler angles estimated using the traditional Kalman filter (up to 90°), thereby yielding comprehensive angle insights. Furthermore, the new sensor alignment technique facilitated posture calculation for the upper body by incorporating the trunk movements

in conjunction with the upper arm and the forearm, thus enhancing the accuracy of the estimation of shoulder and elbow angles and enabling a more accurate ergonomic risk assessment.

This research on large-scale plant nursery workers revealed their significant exposure to extreme postures of the back and the shoulders, especially during the weeding task with high percentage of trunk flexion or lateral bending over 90°, of which the effect could be further amplified by the frequent lifting of heavy loads when these particular workers had to lift the plant containers to clean the area underneath. Ascertaining worker's health and safety by mitigating the risk of musculoskeletal injuries is necessary, and the authors call for the implementation of ergonomic interventions. Once the preventive measures are implemented, our method can serve to reevaluate whether there is an improvement in the posture of the workers.

ACKNOWLEDGMENT

The authors would like to thank all the participants in the study, the Union des producteurs agricoles for connecting them with the plant nursery who allowed them to conduct the fieldwork. They are also thankful the the research assistants, Rebeca Villanueva-Gomez and Mohamed Garouche, for their support during the field data collection. In addition they would like to thank Professor Sheldon Andrews for his suggestions to improve the data analysis and for his support with the use of the MoCap.

REFERENCES

[1] S. Schreven, P. J. Beek, and J. B. J. Smeets, "Optimising filtering parameters for a 3D motion analysis system," *J. Electromyogr. Kinesiol.*, vol. 25, no. 5, pp. 808–814, Oct. 2015.

[2] S.-J. Lee, S. Tak, T. Alterman, and G. M. Calvert, "Prevalence of musculoskeletal symptoms among agricultural workers in the United States: An analysis of the National Health Interview Survey, 2004–2008," *J. Agromedicine*, vol. 19, no. 3, pp. 268–280, Jul. 2014.

[3] J. Lucas, E. Connor, and J. Bose, "Back, lower limb, and upper limb pain among U.S. adults, 2019," Nat. Center Health Statist., Hyattsville, MD, USA, Tech. Rep. 415, 2021. [Online]. Available: https://stacks.cdc.gov/view/cdc/107894

[4] K. Stollenwerk, J. Müllers, J. Müller, A. Hinkenjann, and B. Krüger, "Evaluating an accelerometer-based system for spine shape monitoring," in *Computational Science and Its Applications—ICCSA 2018* (Lecture Notes in Computer Science), O. Gervasi, B. Murgante, S. Misra, E. Stankova, C. M. Torre, A. M. A. Rocha, D. Taniar, B. O. Apduhan, E. Tarantino, and Y. Ryu, Eds., Cham, Switzerland: Springer, 2018, pp. 740–756.

[5] D. I. Rubin, "Epidemiology and risk factors for spine pain," *Neurologic Clinics*, vol. 25, no. 2, pp. 353–371, May 2007.

[6] A. Pourmand, R. AlRemeithi, S. Martinez, C. Couperus, M. Mazer-Amirshahi, J. Yang, and Q. K. Tran, "Cyclobenzaprine utilization for musculoskeletal back pain: Analysis of 2007–2019 National Hospital Ambulatory Medical Care Survey data," *Amer. J. Emergency Med.*, vol. 68, pp. 106–111, Jun. 2023.

[7] D. J. Gaskin and P. Richard, "The economic costs of pain in the United States," *J. Pain*, vol. 13, no. 8, pp. 715–724, Aug. 2012.

[8] D. Hoy, L. March, P. Brooks, F. Blyth, A. Woolf, C. Bain, G. Williams, E. Smith, T. Vos, J. Barendregt, C. Murray, R. Burstein, and R. Buchbinder, "The global burden of low back pain: Estimates from the global burden of disease 2010 study," *Ann. Rheumatic Diseases*, vol. 73, no. 6, pp. 968–974, Jun. 2014.

[9] K. G. Davis and W. S. Marras, "The effects of motion on trunk biomechanics," *Clin. Biomech.*, vol. 15, no. 10, pp. 703–717, Dec. 2000.

[10] K. Walker-Bone, "Musculoskeletal disorders in farmers and farm workers," *Occupational Med.*, vol. 52, no. 8, pp. 441–450, Dec. 2002.

[11] A. J. van der Beek and M. H. Frings-Dresen, "Assessment of mechanical exposure in ergonomic epidemiology," *Occupat. Environ. Med.*, vol. 55, no. 5, pp. 291–299, May 1998.

[12] Y. Roquelaure, C. Ha, C. Rouillon, N. Fouquet, A. Leclerc, A. Descatha, A. Touranchet, M. Goldberg, and E. Imbernon, "Risk factors for upper-extremity musculoskeletal disorders in the working population," *Arthritis Rheumatism*, vol. 61, no. 10, pp. 1425–1434, Oct. 2009.

[13] M. Gómez-Galán, J. Pérez-Alonso, Á.-J. Callejón-Ferre, and J. López-Martínez, "Musculoskeletal disorders: OWAS review," *Ind. Health*, vol. 55, no. 4, pp. 314–337, 2017.

[14] L. McAtamney and E. N. Corlett, "RULA: A survey method for the investigation of work-related upper limb disorders," *Appl. Ergonom.*, vol. 24, no. 2, pp. 91–99, Apr. 1993.

[15] S. Vachinska-Aleksandrova, M. Konsulova-Bakalova, and M. Markov, "An assessment of posture related MSDs risk in university employees using REBA method," in *Proc. Int. Conf. Biomed. Innov. Appl. (BIA)*, vol. 1, Jun. 2022, pp. 99–102.

[16] S. Hignett and L. McAtamney, "Rapid entire body assessment (REBA)," *Appl. Ergonom.*, vol. 31, no. 2, pp. 201–205, Apr. 2000.

[17] M. L. Nunes, D. Folgado, C. Fujão, L. Silva, J. Rodrigues, P. Matias, M. Barandas, A. V. Carreiro, S. Madeira, and H. Gamboa, "Posture risk assessment in an automotive assembly line using inertial sensors," *IEEE Access*, vol. 10, pp. 83221–83235, 2022.

[18] M. R. Kabir, M. A. Jawad, M. Ehsan, H. Mahmud, and M. K. Hasan, "Renovo: Prototype of a low-cost sensor-based therapeutic system for upper limb rehabilitation," 2021, *arXiv:2109.03631*.

[19] D. K. Shaeffer, "MEMS inertial sensors: A tutorial overview," *IEEE Commun. Mag.*, vol. 51, no. 4, pp. 100–109, Apr. 2013.

[20] C. Chen, R. Jafari, and N. Kehtarnavaz, "A survey of depth and inertial sensor fusion for human action recognition," *Multimedia Tools Appl.*, vol. 76, no. 3, pp. 4405–4425, Feb. 2017, doi: 10.1007/s11042-015-3177-1.

[21] V. Vijayan, J. P. Connolly, J. Condell, N. McKelvey, and P. Gardiner, "Review of wearable devices and data collection considerations for connected health," *Sensors*, vol. 21, no. 16, p. 5589, Aug. 2021. [Online]. Available: https://www.mdpi.com/1424-8220/21/16/5589

[22] U. G. Longo, S. De Salvatore, M. Sassi, A. Carnevale, G. De Luca, and V. Denaro, "Motion tracking algorithms based on wearable inertial sensor: A focus on shoulder," *Electronics*, vol. 11, no. 11, p. 1741, May 2022. [Online]. Available: https://www.mdpi.com/2079-9292/11/11/1741

[23] V. M. N. Passaro, A. Cuccovillo, L. Vaiani, M. De Carlo, and C. E. Campanella, "Gyroscope technology and applications: A review in the industrial perspective," *Sensors*, vol. 17, no. 10, p. 2284, Oct. 2017. [Online]. Available: https://www.ncbi.nlm.nih.gov/pmc/articles/PMC5677445/

[24] W. A. Gill, I. Howard, I. Mazhar, and K. McKee, "A review of MEMS vibrating gyroscopes and their reliability issues in harsh environments," *Sensors*, vol. 22, no. 19, p. 7405, Sep. 2022. [Online]. Available: https://www.mdpi.com/1424-8220/22/19/7405

[25] S. Kaji, R. Gando, K. Masunishi, E. Ogawa, F. Miyazaki, H. Hiraga, Y. Tomizawa, and H. Shibata, "A <100 PPB/K frequency-matching temperature stability MEMS rate integrating gyroscope enabled by donut-mass structure," in *Proc. IEEE 33rd Int. Conf. Micro Electro Mech. Syst. (MEMS)*, Jan. 2020, pp. 263–266. [Online]. Available: https://ieeexplore.ieee.org/abstract/document/9056333

[26] A. R. Ranji, V. Damodaran, K. Li, Z. Chen, S. Alirezaee, and M. J. Ahamed, "Recent advances in MEMS-based 3D hemispherical resonator gyroscope (HRG)—A sensor of choice," *Micromachines*, vol. 13, no. 10, p. 1676, Oct. 2022. [Online]. Available: https://www.mdpi.com/2072-666X/13/10/1676

[27] T. Tsukamoto and S. Tanaka, "Rate integrating gyroscope using independently controlled CW and CCW modes on single resonator," *J. Microelectromech. Syst.*, vol. 30, no. 1, pp. 15–23, Feb. 2021. [Online]. Available: https://ieeexplore.ieee.org/abstract/document/9298466

[28] Y. Choi, K. Yoo, S. J. Kang, B. Seo, and S. K. Kim, "Development of a low-cost wearable sensing glove with multiple inertial sensors and a light and fast orientation estimation algorithm," *J. Supercomput.*, vol. 74, no. 8, pp. 3639–3652, Aug. 2018, doi: 10.1007/s11227-016-1833-5.

[29] J. Hislop, M. Isaksson, J. McCormick, and C. Hensman, "Validation of 3-space wireless inertial measurement units using an industrial robot," *Sensors*, vol. 21, no. 20, p. 6858, Oct. 2021. [Online]. Available: https://www.ncbi.nlm.nih.gov/pmc/articles/PMC8537168/

[30] P. Guo, H. Qiu, Y. Yang, and Z. Ren, "The soft iron and hard iron calibration method using extended Kalman filter for attitude and heading reference system," in *Proc. IEEE/ION Position, Location Navigat. Symp.*, May 2008, pp. 1167–1174. [Online]. Available: https://ieeexplore.ieee.org/abstract/document/4570003

[31] L. Ricci, F. Taffoni, and D. Formica, "On the orientation error of IMU: Investigating static and dynamic accuracy targeting human motion," *PLoS ONE*, vol. 11, no. 9, Sep. 2016, Art. no. e0161940. [Online]. Available: https://www.ncbi.nlm.nih.gov/pmc/articles/PMC5017605/

[32] B. Fan, Q. Li, C. Wang, and T. Liu, "An adaptive orientation estimation method for magnetic and inertial sensors in the presence of magnetic disturbances," *Sensors*, vol. 17, no. 5, p. 1161, May 2017. [Online]. Available: https://www.mdpi.com/1424-8220/17/5/1161

[33] P. Daponte, L. De Vito, S. Rapuano, M. Riccio, and F. Picariello, "Compensating magnetic disturbances on MARG units by means of a low complexity data fusion algorithm," in *Proc. IEEE Int. Symp. Med. Meas. Appl. (MeMeA)*, May 2015, pp. 157–162.

[34] N. Yadav and C. Bleakley, "Accurate orientation estimation using AHRS under conditions of magnetic distortion," *Sensors*, vol. 14, no. 11, pp. 20008–20024, Oct. 2014. [Online]. Available: https://www.mdpi.com/1424-8220/14/11/20008

[35] Z. Wang, H. Zhao, S. Qiu, and Q. Gao, "Stance-phase detection for ZUPT-aided foot-mounted pedestrian navigation system," *IEEE/ASME Trans. Mechatronics*, vol. 20, no. 6, pp. 3170–3181, Dec. 2015.

[36] H. Lim, B. Kim, and S. Park, "Prediction of lower limb kinetics and kinematics during walking by a single IMU on the lower back using machine learning," *Sensors*, vol. 20, no. 1, p. 130, Dec. 2019. [Online]. Available: https://www.mdpi.com/1424-8220/20/1/130

[37] B. Han, Y. Jiao, G. Liu, L. Zhang, Q. Zhu, Y. Yan, and J. Fei, "Kinematic & dynamic models of human lower extremity during the gait cycle," in *Proc. 6th Int. Conf. Control, Autom. Robot. (ICCAR)*, Apr. 2020, pp. 568–573.

[38] R. Caldas, M. Mundt, W. Potthast, F. B. de Lima Neto, and B. Markert, "A systematic review of gait analysis methods based on inertial sensors and adaptive algorithms," *Gait Posture*, vol. 57, pp. 204–210, Sep. 2017.

[39] W. Li, R. Chen, Y. Yu, Y. Wu, and H. Zhou, "Pedestrian dead reckoning with novel heading estimation under magnetic interference and multiple smartphone postures," *Measurement*, vol. 182, Sep. 2021, Art. no. 109610. [Online]. Available: https://www.sciencedirect.com/science/article/pii/S0263224121005832

[40] H. Chen, M. C. Schall, and N. B. Fethke, "Measuring upper arm elevation using an inertial measurement unit: An exploration of sensor fusion algorithms and gyroscope models," *Appl. Ergonom.*, vol. 89, Nov. 2020, Art. no. 103187.

[41] H. Chen, M. Schall, and N. Fethke, "Effects of movement speed and magnetic disturbance on the accuracy of inertial measurement units," in *Proc. Hum. Factors Ergonom. Soc. Annu. Meeting*, vol. 61, 2017, pp. 1046–1050.

[42] S. O. H. Madgwick. (2010). *An Efficient Orientation Filter for Inertial and Inertial/magnetic Sensor Arrays*. [Online]. Available: https://api.semanticscholar.org/CorpusID:2976407

[43] S. O. H. Madgwick, A. J. L. Harrison, and R. Vaidyanathan, "Estimation of IMU and MARG orientation using a gradient descent algorithm," in *Proc. IEEE Int. Conf. Rehabil. Robot.*, Jun. 2011, pp. 1–7.

[44] Y. Zhu, "Posture calculation of improved complementary filtering algorithm based on quaternion," in *Proc. 2nd Int. Symp. Comput. Eng. Intell. Commun. (ISCEIC)*, Aug. 2021, pp. 38–43.

[45] Y. Liu, X. Tian, and X. Xu, "Posture estimation system by IMM-based unscented Kalman filters," in *Proc. Chin. Autom. Congr. (CAC)*, Oct. 2017, pp. 2363–2368.

[46] A. Saito, S. Kizawa, Y. Kobayashi, and K. Miyawaki, "Pose estimation by extended Kalman filter using noise covariance matrices based on sensor output," *ROBOMECH J.*, vol. 7, no. 1, p. 36, Oct. 2020, doi: 10.1186/s40648-020-00185-y.

[47] K. Kitano, A. Ito, and N. Tsujiuchi, "Hand motion measurement using inertial sensor system and accurate improvement by extended Kalman filter," in *Proc. 41st Annu. Int. Conf. IEEE Eng. Med. Biol. Soc. (EMBC)*, Jul. 2019, pp. 6405–6408.

[48] Y. Huang, J. Gong, T. Yao, C. Wang, Y. Jin, and G. Shi, "High accuracy extend Kalman filter for posture measurement based on attitude and heading reference system," in *Proc. IEEE Int. Conf. Real-Time Comput. Robot. (RCAR)*, Jul. 2017, pp. 262–266.

[49] S. O. H. Madgwick, "An efficient orientation filter for inertial and inertial/magnetic sensor arrays," Dept. Mech. Eng., Univ. Bristol, Bristol, U.K., Tech. Rep., 2010.

[50] X. Yuan, S. Yu, S. Zhang, G. Wang, and S. Liu, "Quaternion-based unscented Kalman filter for accurate indoor heading estimation using wearable multi-sensor system," *Sensors*, vol. 15, no. 5, pp. 10872–10890, May 2015.

[51] D. V. A. N. R. Kumar, S. K. Rao, and K. P. Raju, "Integrated unscented Kalman filter for underwater passive target tracking with towed array measurements," *Optik*, vol. 127, no. 5, pp. 2840–2847, Mar. 2016.

[52] R. R. Labbe Jr., *Kalman and Bayesian Filters in Python*. San Francisco, CA, USA: GitHub, 2020.

[53] D. Ebeigbe, T. Berry, M. M. Norton, A. J. Whalen, D. Simon, T. Sauer, and S. J. Schiff, "A generalized unscented transformation for probability distributions," 2021, *arXiv:2104.01958*.

[54] E. A. Wan and R. Van Der Merwe, "The unscented Kalman filter for nonlinear estimation," in *Proc. IEEE Adapt. Syst. Signal Process., Commun., Control Symp.*, Oct. 2000, pp. 153–158.

[55] T. Beravs, P. Reberšek, D. Novak, J. Podobnik, and M. Munih, "Development and validation of a wearable inertial measurement system for use with lower limb exoskeletons," in *Proc. 11th IEEE-RAS Int. Conf. Humanoid Robots*, Oct. 2011, pp. 212–217.

[56] C. Naab and Z. Zheng, "Application of the unscented Kalman filter in position estimation a case study on a robot for precise positioning," *Robot. Auto. Syst.*, vol. 147, Jan. 2022, Art. no. 103904.

[57] R. Villanueva-Gómez, O. Thamsuwan, R. A. Barros-Castro, and L. H. Barrero, "Seasonal migrant workers perceived working conditions and speculative opinions on possible uptake of exoskeleton with respect to tasks and environment: A case study in plant nursery," *Sustainability*, vol. 15, no. 17, p. 12839, Aug. 2023. [Online]. Available: https://www.mdpi.com/2071-1050/15/17/12839

[58] C. Z. Shan, S. L. Sen, Y. C. Fai, and E. S. L. Ming, "Investigation of sensor-based quantitative model for badminton skill analysis and assessment," *Jurnal Teknologi*, vol. 72, no. 2, pp. 93–96, Jan. 2015.

[59] R. Valenti, I. Dryanovski, and J. Xiao, "Keeping a good attitude: A quaternion-based orientation filter for IMUs and MARGs," *Sensors*, vol. 15, no. 8, pp. 19302–19330, Aug. 2015.

[60] M. Kok, J. D. Hol, and T. B. Schön, "Using inertial sensors for position and orientation estimation," *Found. Trends Signal Process.*, vol. 11, nos. 1–2, pp. 1–153, 2017.

[61] M. Gan, S. M. V. Liang, A. M. M. Obciana, C. J. G. Policarpio, and H. S. Co, "Accelerometer ranges for different static postures," in *Proc. IEEE 10th Int. Conf. Humanoid, Nanotechnol., Inf. Technol., Commun. Control, Environ. Manage. (HNICEM)*, Nov. 2018, pp. 1–6.

[62] T. Marcard, B. Rosenhahn, M. Black, and G. Pons-Moll, "Sparse inertial poser: Automatic 3D human pose estimation from sparse IMUs," *Comput. Graph. Forum*, vol. 36, no. 2, pp. 349–360, 2017.

[63] O. Thamsuwan, K. Galvin, M. Tchong-French, J. H. Kim, and P. W. Johnson, "A feasibility study comparing objective and subjective field-based physical exposure measurements during apple harvesting with ladders and mobile platforms," *J. Agromedicine*, vol. 24, no. 3, pp. 268–278, Jul. 2019.

[64] O. Thamsuwan, K. Galvin, M. Tchong-French, L. Aulck, L. N. Boyle, R. P. Ching, K. J. McQuade, and P. W. Johnson, "Comparisons of physical exposure between workers harvesting apples on mobile orchard platforms and ladders. Part 1: Back and upper arm postures," *Appl. Ergonom.*, vol. 89, Nov. 2020, Art. no. 103193. [Online]. Available: https://www.sciencedirect.com/science/article/pii/S0003687020301460

[65] B. Ge, H. Zhang, L. Jiang, Z. Li, and M. M. Butt, "Adaptive unscented Kalman filter for target tracking with unknown time-varying noise covariance," *Sensors*, vol. 19, no. 6, p. 1371, Mar. 2019.

[66] M. M. Rahman, K. B. Gan, N. A. A. Aziz, A. Huong, and H. W. You, "Upper limb joint angle estimation using wearable IMUs and personalized calibration algorithm," *Mathematics*, vol. 11, no. 4, p. 970, Feb. 2023.

[67] X. Li, M. Chen, and L. Zhang, "Quaternion-based robust extended Kalman filter for attitude estimation of micro quadrotors using low-cost MEMS," in *Proc. 35th Chin. Control Conf. (CCC)*, Jul. 2016, pp. 10712–10717.

[68] L. Ji, H. Wang, T. Zheng, and X. Qi, "Motion trajectory of human arms based on the dual quaternion with motion tracker," *Multimedia Tools Appl.*, vol. 76, no. 2, pp. 1681–1701, Jan. 2017.

[69] Y. Xiaoping, E. R. Bachmann, and R. B. McGhee, "A simplified quaternion-based algorithm for orientation estimation from Earth gravity and magnetic field measurements," *IEEE Trans. Instrum. Meas.*, vol. 57, no. 3, pp. 638–650, Mar. 2008.
[70] K. Xiong, H. Y. Zhang, and C. W. Chan, "Performance evaluation of UKF-based nonlinear filtering," *Automatica*, vol. 42, no. 2, pp. 261–270, Feb. 2006.
[71] R. Mehrizi, X. Peng, X. Xu, S. Zhang, D. Metaxas, and K. Li, "A computer vision based method for 3D posture estimation of symmetrical lifting," *J. Biomech.*, vol. 69, pp. 40–46, Mar. 2018.
[72] L. Liu, Q. Hu, and F. Mei, "Dynamic IMU calibration in IMU-MoCap on lower limbs based on joint constraints," in *Proc. 5th Int. Conf. Commun. Inf. Syst. (ICCIS)*, Oct. 2021, pp. 180–184.
[73] A. Yazdani, R. S. Novin, A. Merryweather, and T. Hermans, "Is the leader robot an adequate sensor for posture estimation and ergonomic assessment of a human teleoperator?" in *Proc. IEEE 17th Int. Conf. Autom. Sci. Eng. (CASE)*, Aug. 2021, pp. 1946–1952.
[74] M. I. Khan, B. Bath, A. Kociolek, X. Zeng, N. Koehncke, and C. Trask, "Trunk posture exposure patterns among Prairie ranch and grain farmers," *J. Agromedicine*, vol. 25, no. 2, pp. 210–220, Apr. 2020.
[75] N. B. Fethke, M. C. Schall, H. Chen, C. A. Branch, and L. A. Merlino, "Biomechanical factors during common agricultural activities: Results of on-farm exposure assessments using direct measurement methods," *J. Occupat. Environ. Hygiene*, vol. 17, nos. 2–3, pp. 85–96, Mar. 2020.
[76] R. F. Granzow, M. C. Schall, M. F. Smidt, H. Chen, N. B. Fethke, and R. Huangfu, "Characterizing exposure to physical risk factors among reforestation hand planters in the southeastern United States," *Appl. Ergonom.*, vol. 66, pp. 1–8, Jan. 2018.
[77] W. Lee, J.-H. Lin, N. Howard, and S. Bao, "Physiological responses, trunk posture, and work pace in commercial building cleaning in Washington state: An observational field study," *J. Saf. Res.*, vol. 86, pp. 107–117, Sep. 2023. [Online]. Available: https://www.sciencedirect.com/science/article/pii/S002243752300066X
[78] X. Li, C. Zhang, Y. Zheng, and N. Zhang, "A novel constrained UKF method for both updating structural parameters and identifying excitations for nonlinear structures," *Soil Dyn. Earthq. Eng.*, vol. 158, Jul. 2022, Art. no. 107291.
[79] N. D. Nath, R. Akhavian, and A. H. Behzadan, "Ergonomic analysis of construction worker's body postures using wearable mobile sensors," *Appl. Ergonom.*, vol. 62, pp. 107–117, Jul. 2017. [Online]. Available: https://www.sciencedirect.com/science/article/pii/S0003687017300339

AMINE ZOUGALI received the M.Sc. degree in power systems from the University of Sciences and Technology Houari Boumediene, Algiers, in June 2020, and the M.Sc. degree in engineering, renewable energies, and energy efficiency from École de Technologie Supérieure, Montreal, in July 2023. He currently works as a Research Assistant with the Department of Mechanical Engineering, École de Technologie Supérieure. His research interest includes developing an algorithm for estimating human body postures.

ORNWIPA THAMSUWAN received the B.Eng. degree in industrial engineering from Chulalongkorn University, Bangkok, in 2008, and the M.Sc. and Ph.D. degrees in industrial engineering from the University of Washington, Seattle, in 2011 and 2016, respectively. She currently works as an Associate Professor with École de Technologie Supérieure. In July 2021, she started a research program in the user-centered design of wearable assistive devices. Her research interests include field-based characterization of human posture using IMU, muscle activity with EMG, and cognitive stress through heart rate variability.